



## AN AMPEROMETRIC AQUEOUS ETHANOL SENSOR BASED ON THE ELECTROCATALYTIC OXIDATION AT A COBALT-NICKEL OXIDE ELECTRODE

ERIC T. HAYES,\*† BRYANT K. BELLINGHAM,\* HARRY B. MARK, Jr\* and AHMED GALAL†

\* Department of Chemistry, University of Cincinnati, Cincinnati, OH 45221, U.S.A.

† Department of Chemistry, College of Science, University of Cairo, Giza, Egypt

(Received 1 August 1994; in revised form 19 October 1994)

**Abstract**—An electrodeposited mixed oxide film of Co–Ni has been applied as a sensor for the amperometric determination of aqueous ethanol samples. The electrode has a linear response over a 1.5–7.9 mM ethanol concentration range with a detection limit of 32  $\mu$ M ethanol. Deposition conditions for maximum catalytic efficiency, electrode lifetime and optimum analytical analysis potential are discussed. SEM, EDAX and electrochemical kinetic studies indicate that the active catalytic species in the electrode film is a 2:1 Co–Ni oxide species and suggest a partial mechanism of the ethanol oxidation reaction. The feasibility of this modified electrode for the determination of atmospheric ethanol is also examined. All other organic alcohols tested were interferents. Conditions affecting the stability of the sensor are discussed.

**Key words:** ethanol sensor, Co–Ni mixed oxides, electrocatalysis, electrooxidation, amperometry, modified electrodes.

### INTRODUCTION

The direct determination of ethanol in aqueous solution by electroanalysis with conventional metal and carbon electrodes is virtually impossible. Because of the large overpotential for the oxidation of ethanol, virtually no appreciable reaction is obtained without the presence of a catalyst and, even so, fouling of the electrode surface by oxidation products generally occurs[1, 2]. Furthermore, the need for high applied potentials results in interference by the simultaneous oxidation of other species usually present in typical sample systems[3, 4]. This requires selectivity for the oxidation reaction for a practical sensor. Thus, it is generally necessary to use a modified electrode system which has selective electrocatalytic properties.

The most common approach to the electroanalysis of aqueous ethanol employs enzyme modified electrodes which incorporate either alcohol dehydrogenase (ADH) or alcohol oxidase (AO)[5, 6]. These enzymes convert either directly or indirectly the ethanol into electroactive products such as  $\text{NADH}^+$ ,  $\text{H}_2\text{O}_2$ , and  $\text{O}_2$  which are subsequently determined electrochemically. In some cases, the enzymes are immobilized on a column reactor in a flow system and the products determined at an upstream electrode[7]. In other cases, the enzymes are immobilized, by a wide variety of methods, on the electrode surface[8, 9].

In addition to enzymes, other materials, for example, metals (Ir, Ni) alloys (PtSn, NiMo), oxides and mixed oxides [ $\text{PbO}_2$ ,  $\text{TiO}_3$ ,  $\text{Ni}(\text{OH})_2$ ,  $\text{NiCO}_2\text{O}_4$  and  $\text{CrO}_3:\text{TiO}_3:\text{Sb}_2\text{O}_3$ ] and metal complexes (phthalocyanines, porphyrins, peroskites, and tetraazomacrocyclics), have been used as electrodes for the electrocatalytic oxidation of alcohols in synthetic and fuel cell applications[10–21]. All of the above electrode materials, except the pure metals, have transition metal ion centers which have either unpaired *d*-electrons or empty *d*-orbitals available for bond formation with adsorbed alcohol and/or redox intermediates. The metal ion center can undergo changes in its oxidation state in the course of alcohol oxidation reaction[22, 23]. Other factors that influence the selectivity, stability and kinetics of the electrooxidation of alcohols by these materials are geometric arrangement of the atoms on the surface, surface area, catalyst support material, grain boundaries and surface morphology (lattice defects) on an atomic dimension[24–28].

Although these non-conventional electrode materials have been developed primarily for large scale electrosyntheses, industrial processes, and fuel cell applications, their potential for application as electrodes for specific organic sensors is enormous. As a previous publication has described the use of Co–Ni mixed oxides as an electrode for the catalytic oxidation of ethanol to acetic acid[29], this paper described the design, characteristics and performance of this mixed oxide electrode as a selective sensor for aqueous (and atmospheric) ethanol.

† Author to whom correspondence should be addressed.

## EXPERIMENTAL

### Solutions

All solutions were made with distilled water that was passed through a Sybron-Barnsted NANO Pure II System. All chemicals were reagent grade. Stock solutions of ethanol (absolute) ranging from 0.01% (v/v) to 10% (v/v) were also 2.5 M in KOH as were the 10% stock solutions of methanol, propanol, butanol and benzyl alcohol.

### Instrumentation

All electrochemical experiments were carried out in a standard 25 ml three compartment cell using a platinum disc electrode (1.35 mm), BAS Model MF 2013) as the working electrode, an Ag-AgCl reference electrode, and a platinum wire coil as the auxiliary electrode. The mixed oxide electrodeposition and cyclic voltammetry studies were carried out with a BAS 100 Electrochemical Analyzer. The amperometric analyses of ethanol were carried out using a BAS CV-1B potentiostat and the applied potential was monitored by a Keithley 179A TRMS Multimeter. The resulting current-time plots were recorded on a Fisher Recordall series 5000. The scanning electron microscopy (SEM) was a Cambridge Stereoscan 600 and EDAX spectra were obtained with a Cambridge 100 X-Ray Instrument with a Cambridge Model 2P goniometer and a cobalt anticathode.

### Experimental procedures

The mixed oxide film was electrodeposited on the Pt disk from mixed cobalt-nickel nitrate solutions at a constant applied potential of  $-2.00$  V. The deposition time was varied from 30 to 300 s. This modified electrode was placed directly in the electrolysis cell containing 15 ml of the stirred 2.5 M KOH solution after pretreatment at  $+0.270$  V for 2 h in 146 mM ethanol-2.5 M KOH. A constant applied potential of  $+0.270$  V was used throughout all analytical measurements. Ethanol samples from the various stock solutions were injected (1400  $\mu$ l) and the  $i-t$  curves were recorded on each injection. All experiments were carried out at room temperature and the solutions were not deaerated.

"Atmospheric" ethanol samples were generated by bubbling a constant flow (100 ml min<sup>-1</sup>) of argon through 1%, 5% and 10% (v/v) ethanol solutions. The resulting ethanol-argon vapor was then bubbled continuously in the 2.5 M KOH electrolyte solution for two minutes in the electrolysis cell and the  $i-t$  curves recorded.

## RESULTS AND DISCUSSION

### Electrode optimization

Various parameters such as the ratio and total concentration of Co-Ni in the deposition solution, deposition potential and time, and electrode storage conditions were varied in order to optimize the sensitivity, response time, reproducibility, stability, and the dynamic range of this mixed-oxide electrode for the analysis of aqueous ethanol solutions.

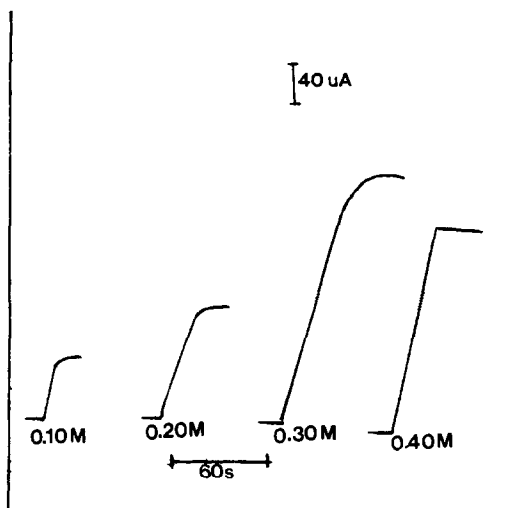


Fig. 1.  $i-t$  curves for a 146 mM ethanol-2.5 M KOH of total Co-Ni deposition solution concentrations: 0.10 M, 0.20 M, 0.30 M, 0.40 M; 1:1 Co-Ni concentration ratio and detector,  $E_{app} = +0.270$  V.

*Variation of Co-Ni ratio and total concentration in deposition solutions.* In previous reports on the use of cobalt-nickel mixed oxide (spinel) electrodes for the oxidation of ethanol to acetic acid, the oxide film was prepared by spray coating the oxide mixture on a titanium substrate followed by high temperature treatment[30-32]. A crystalline structure with a composition of  $NiCo_2O_4$  was found. However, no direct determination of the actual valences of the active material was performed. As this procedure for the formation of the active electrode is both time consuming and laborious, this study formed the film by simple electrochemical deposition alone.

Initial studies employed deposition solutions with an equimolar concentration ratio of Co-Ni and total concentrations ranging from 0.10 to 0.40 M with an applied potential of  $-2.00$  V for 180 s using a platinum disk as the deposition substrate. Figure 1 shows that the limiting or steady-state current of the  $i-t$  curves for the injection of a 146 mM ethanol sample increases as the total concentration of the deposition mixture increased from 0.1 to 0.3 M and then decreased as the deposition mixture concentration was increased further. As the spacial arrangement of the catalyst atoms is important in surface reactions that involve adsorption steps in the mechanism[31], this concentration of the deposition mixture might produce an optimum configuration of the active surface atoms with respect to the adsorbate.

With respect to the effect of the Co-Ni ratio in the deposition mixture (total concentration 0.3 M and 180 s deposition time), Fig. 2 shows that the maximum steady-state current is obtained at an approximate 2:1 Co-Ni ratio in the deposition mixture.

*Effect of film deposition time.* The film deposition time, using an equimolar Co-Ni ratio of 0.3 M concentration, was varied from 30 to 300 s. The limiting currents for the injection of 146 mM ethanol are shown in Fig. 3. It can be seen that the current increases as the deposition time increases from 30 to

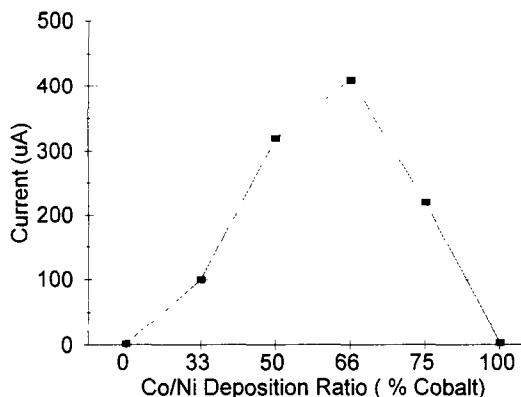


Fig. 2. Plot of current response vs. Co-Ni deposition solution ratio: 0-100% cobalt; 146 mM ethanol-2.5 M KOH, 0.30 M total concentration Co-Ni,  $E_{app} = +0.270$  V.

180 s and then rapidly decreases at higher deposition times. This decrease might result from increasing resistance in the thicker films. Although the maximum sensitivity is obtained for a 180 s deposition time, the  $i-t$  curves of Fig. 3 shows that the maximum response rise time is obtained for a 60 s deposition time which is somewhat advantageous for the analysis of low ethanol concentrations.

**Electrode stability.** Stability (or lifetime) is an important prerequisite for a practical sensor. Initial analytical studies showed that individual electrodes exhibited as much as 60% decrease in response on overnight storage in  $H_2O$ , 2.5 M KOH, 146 mM alcohol-2.5 M KOH solutions, or air between continuous uses. Also, SEM pictures showed large changes in the surface morphology occurred during storage discussed in a subsequent section. Conditions that resulted in more stable storage and extended the lifetime of the electrode were determined.

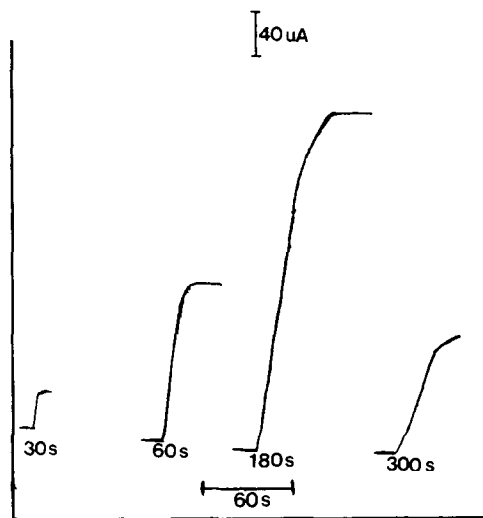


Fig. 3.  $i-t$  curves of varying deposition time: 30-300 s, at  $-2.00$  V; 146 mM ethanol-2.5 M KOH,  $E_{app} = +0.270$  V, 0.30 M total concentration Co-Ni.

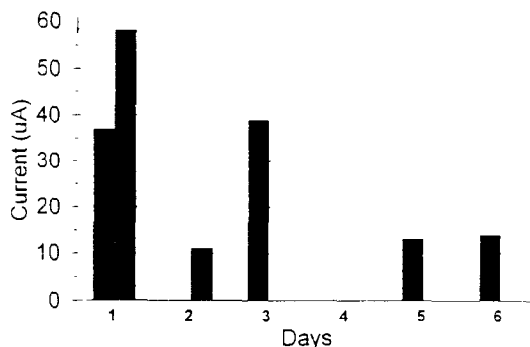


Fig. 4. Stability test plot: (■) dynamic storage, (■) rest storage.

Visual observations showed that the oxide film decomposed on the above storage conditions but it did not occur during the periods of analytical measurements. This suggested that a reduction of the valence state of one or both metals on storage produced oxide(s) that were chemically unstable. Thus, the electrodes were stored in 146 mM ethanol-2.5 M KOH with an applied potential of  $+0.270$  V. (This potential was chosen as it is the initial potentiometric rest potential in this solution). Also, freshly deposited electrodes were pretreated using these conditions prior to analytical use. Figure 4 shows the results obtained for a typical fresh pretreated electrode used to analysis repetitive 146 mM ethanol-2.5 M KOH solutions over a period of 6 days. Each analysis was carried out with a new sample solution. There were 30 replicate samples on day 1, 25 on day 3, 10 on day 5 and 5 on day 6. The electrode was stored as described above with an applied potential between run periods. It can be seen that the electrode response over the first three days is essentially constant but drops off about 50% on days 5 and 6. It is important to note that the current during storage between day 1 and day 3 remained constant during this entire period. In contrast, Fig. 4 also shows the results for the same sample solution using another pretreated electrode which was stored overnight in 2.5 M KOH with no applied potential. On the second day the electrode response was about 70% less. The width of the bars indicate the approximate time period of analyses on each day. Thus, it is apparent that storage under an applied potential maintains the valences of the metal ions in the oxide film at an oxidation state which produces the catalysis compound in a chemically stable form. The electrode pretreatment procedure was found to produce electrodes that reached stable responses after about three or four initial runs. Without this pretreatment, responses were erratic for 20-30 runs before reaching stable values.

**Electrodeposition and analysis applied potentials:** Although the applied deposition potential of  $-2.00$  V is well into the  $H_2$  evolution range for a Pt electrode, it was found that stable and adherent films (presumably metallic at this potential) were obtained but were not formed when lower potentials were applied. The mixed oxides of these metal films are thought to form when the electrode is placed in the 2.5 M KOH electrolyte solution and the  $+0.250$  V

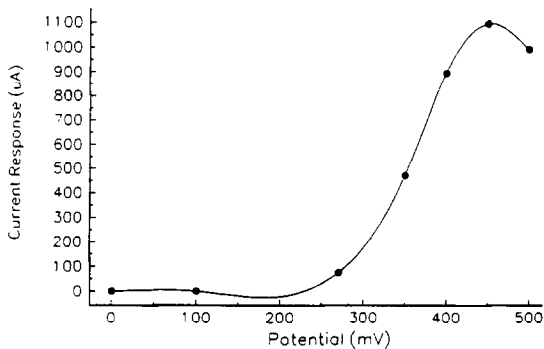


Fig. 5. Hydrodynamic voltammogram of a 146 mM ethanol-2.5 M KOH solution.

analysis potential or +0.270 V pretreatment potential is applied prior to sample ethanol injections. With respect to the analysis applied potential; for a 146 mM ethanol sample in 2.5 M KOH, Fig. 5 shows that the current rises sharply starting at about +0.20 V and reaches a maximum value at about +0.44 V. An applied potential of +0.270 V (at the foot of the voltammogram) was chosen for the amperometric analysis, *not* to obtain maximum sensitivity, but to minimize potential interference from other oxidizable species expected to be in real samples.

*Analytical measurements.* Typical current-time response for successive additions of 1400  $\mu$ l of a 1% ethanol stock solution to 15 ml of 2.5 M KOH electrolyte in the cell are shown in Fig. 6. The total ethanol concentration after each addition is shown

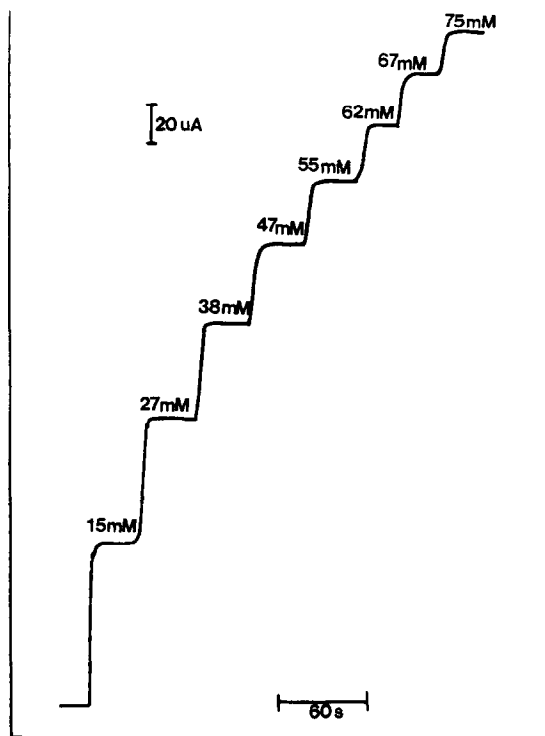


Fig. 6. *I-t* of calibration plot: successive ethanol additions (15-70 mM).

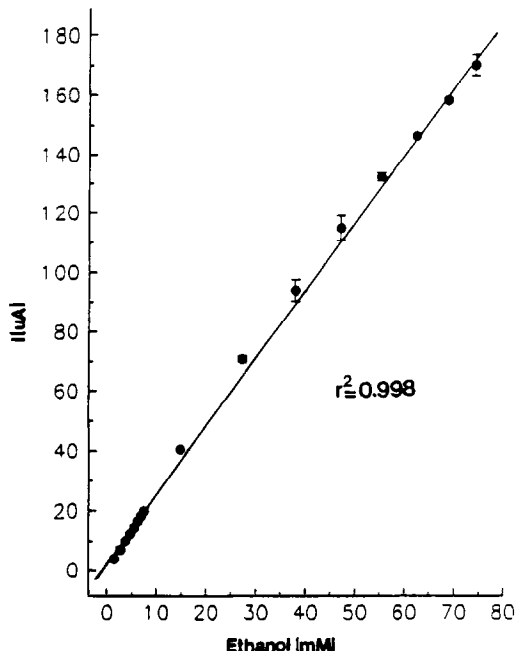


Fig. 7. Ethanol calibration plot (1.5-79 mM).

above the steady state limiting currents. Figure 7 shows a typical calibration curve constructed from the above type curves. Each concentration point in Fig. 7 represents the average and error bars for at least four replicate runs. Although the plot is slightly curved, which is real, it is virtually linear over a concentration range from 1.5 mM to 79 mM ( $r^2 = 0.998$ ). The portion of the plot from 1.5 ml to 7.5 mM is expanded in Fig. 8 and shows greater linearity

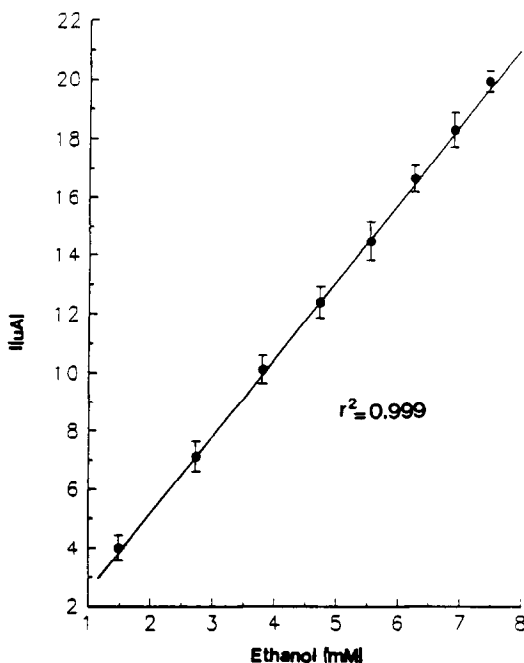


Fig. 8. Ethanol calibration plot (1.5 M-79 mM)

Table 1. Interferent results

Alcohols (106 mM)	$i$ ( $\mu$ A)	Alcohol (53 mM) + ethanol (53 mM) $i$ ( $\mu$ A)*
Benzyl	91	106
Butanol	54	85
Ethanol†	89	—
Methanol	72	86
Propanol	73	100

\* 53 mM ethanol 70  $\mu$ A.

† Current exceeds all other alcohols except benzyl.

( $r^2 = 0.999$ ). The detection limit for these experimental conditions is  $32 \mu\text{m}$  (based on 3 s/M criteria[33]).

**Interferent studies.** The following alcohols were tested as possible interferents: 1-butanol, benzyl alcohol, methanol and 1-propanol. Each of these alcohols (106 mM) gave significant currents under analysis conditions and gave significant interference when mixed in 1:1 concentrations with ethanol (53 mM each). The results are shown in Table 1. Thus, it is concluded that this Co-Ni mixed oxide sensor is *not-specific* for ethanol but did give lower responses of other alcohols when tested alone. It is safe to assume that any other species that is oxidized at the sensor applied potential will be an interferent.

**"Atmospheric" ethanol.** A preliminary study was made to test the feasibility of adapting this Co-Ni mixed oxide electrode as a sensor for atmospheric ethanol samples. In these experiments the argon stream, previously bubbled through 1%, 5% and 10% aqueous ethanol solutions (partial pressures of ethanol are 49, 198 and 370 mm, respectively) was passed over the 2.5 M KOH electrolyte solution in the cell for 2 min and the resulting  $i-t$  curves recorded as shown in Fig. 9A. In each case the current rises exponentially and appears to approach a steady-state current. Using an integral fixed-time kinetic analysis technique[34], the currents at  $t_f$  were essentially directly proportional to concentration of the ethanol in the bubbler as shown in Fig. 9B. The development of an atmospheric ethanol sensor is now in progress.

#### Mechanism studies

In an effort to determine the causes of the response and stability characteristics and to identify the catalytic active species in the mixed oxide film, EDAX, SEM, and electrochemical studies were carried out.

**EDAX and SEM surface characterization.** EDAX spectra of the mixed oxide films prepared by electro-deposition at  $-2.00$  V for 60 s and with three different deposition solutions (0.3 M total conc.): (i) 1:1 Co-Ni ratio; (ii) 1:2 Co-Ni ratio, and (iii) 2:1 Co-Ni ratio were determined. For each ratio, one film was simply air-dried for 24 h and one was soaked in 146 mM ethanol-2.5 M KOH (1 h) and then air-dried. Table 2 shows the Co-Ni ratio obtained from the EDAX spectra of each pair of films. One conclusion can be reached from these spectra. Regardless of the initial Co-Ni ratio in the deposition solution, the resulting films tend to a 2:1 Co-Ni composition. This suggests that the electro-

Table 2. Comparison of the [Co]-[Ni] ratio in the deposition solution to that of the electrodeposited film (a) before and (b) after exposure to ethanol (146 mM)

[Co]-[Ni] deposition solution	[Co]-[Ni] electrode film
0.5	(a) 2.1
	(b) 2.2
1.0	(a) 1.7
	(b) 1.1
2.0	(a) 2.3
	(b) 2.2

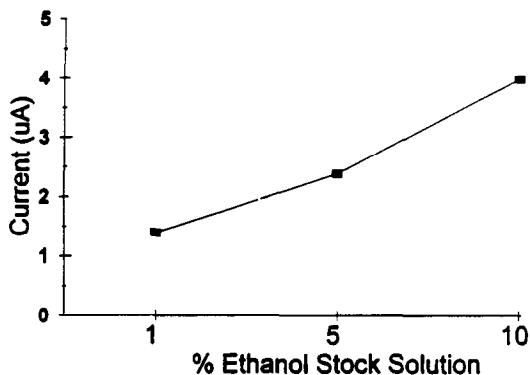
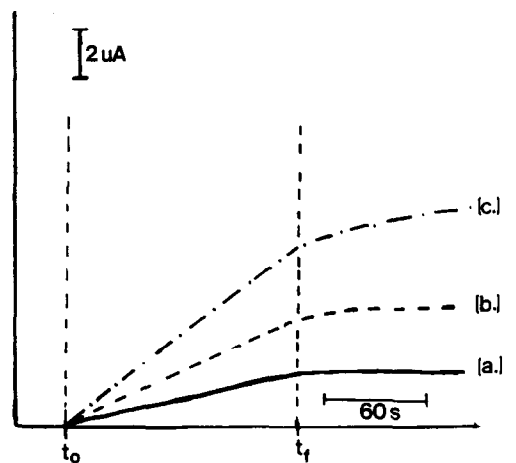


Fig. 9. (A)  $I-t$  response to "atmospheric" ethanol: (a) 1%, (b) 5% and (c) 10% ethanol in bubbler; (B) "atmospheric" ethanol calibration plot (1-10% ethanol bubbler).



Fig. 10. SEM of (A) unexposed Co-Ni oxide film and (B) film exposed to 146 mM–2 M KOH.

deposition eventually forms the same catalytically active or similar  $\text{NiCo}_2\text{O}_4$  species that was previously demonstrated in the high temperature preparation [30, 32].

With respect to SEM studies, these consistently show distinct differences between the unexposed and ethanol exposed films. Figure 10 shows a typical pair. Both surfaces have large cracks in the flat film matrix. However, the unexposed film (Fig. 10A) is

covered by numerous small crystallites scattered on the surface. After exposure to ethanol (Fig. 10B), these small crystallites have been dissolved off the flat oxide surface. The cracks are essentially unchanged. This observation may explain why unpretreated oxide electrodes give erratic current response for the first 20 or so replicate runs and the pretreated electrodes are reproducible after only a few runs.

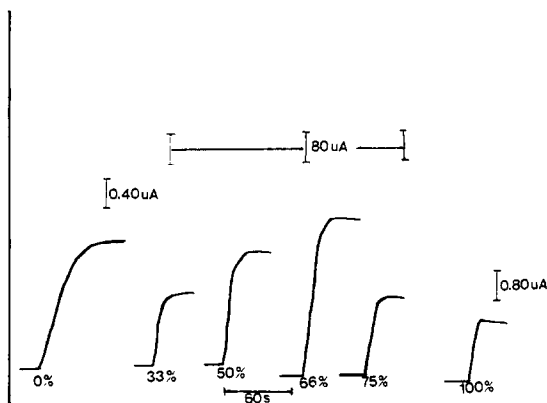


Fig. 11.  $I-t$  curves of film formed on deposition from various Co-Ni solutions.

**Electrochemical kinetic studies.** The current-time curves for 146 mM ethanol-2, 5 M KOH obtained with films formed on the deposition from 0.3 M solutions of  $\text{Co}^{+2}$ , 1:2 Co-Ni, 1:1 Co-Ni, 2:1 Co-Ni, 3:1 Co-Ni and  $\text{Ni}^{+2}$  are shown in Fig. 11. The steady-state current obtained is smallest for the pure metal films and reaches a maximum for the film electrodeposition from 2:1 Co-Ni solution (also plotted in Fig. 2). An assumption that these steady state currents are kinetic rather than diffusion limited (also discussed below in the cyclic voltammetry experiment) is supported by the same trend in rise times to the steady state values shown in Fig. 11. This further supports the concept that the most active catalyst is some 2:1 Co-Ni species in the electrodeposited films.

The cyclic voltammograms (CV's) for oxide film of Co, Ni and 2:1 deposited Co-Ni are given in Fig. 12A, B and C, respectively. These figures also show the CV's for each in the presence (curve 1) and absence (curve 2) of 146 mM ethanol. Figure 12A in the absence of alcohol (curve 2) shows a slightly irreversible cobalt redox couple in the film with an anodic current peak at about +0.27 V. The nickel film, Fig. 12B, curve 2, shows a somewhat more irreversible couple with an anodic peak potential at +0.33 V. In the mixed oxide film (Fig. 12c), curve 2, the nickel and cobalt couple have merged into simple broad anodic and cathodic waves with a peak anodic current at +0.24 V and cathodic peak at about +0.12 V. With ethanol present (Fig. 12A and B) both the Co anodic peak current and the Ni peak current (curves 1) show a small increase with no significant shift of the peak potentials. All three films show a large broad totally irreversible ethanol peak at about +0.43 V. The scan rate dependence of the mixed oxide film in the presence of ethanol can be seen in Fig. 13. It is interesting to note that the reverse peak at +0.43 V increases positive with increasing scan rate. This indicates that the ethanol anodic process is kinetic and ethanol adsorption controlled[35]. The decrease in both the forward and reverse peak at potentials greater than +0.43 V is the result of potential driven desorption of ethanol with increasing positive potential. This also explains the unusual decrease in current of higher positive

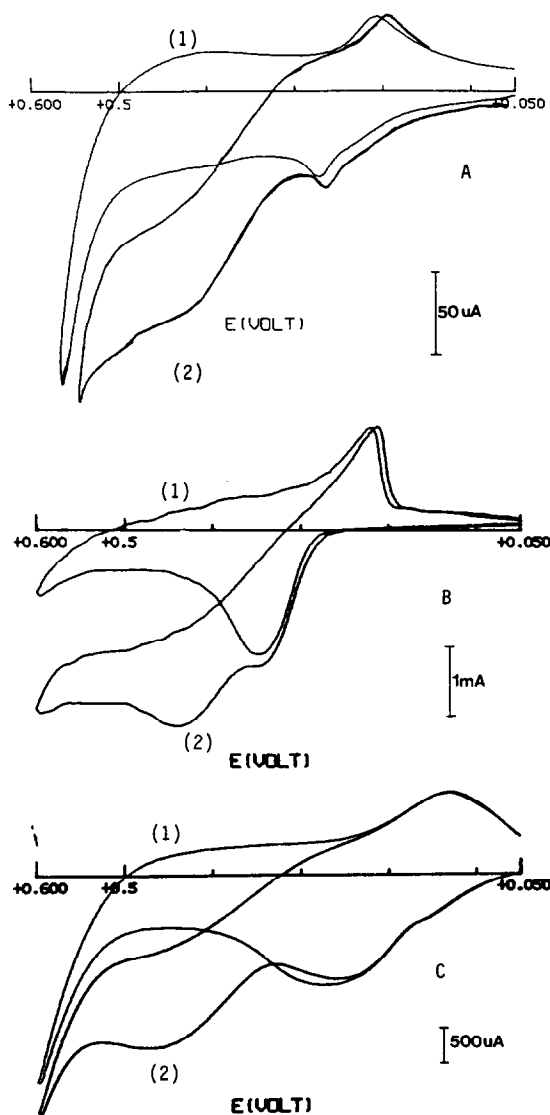


Fig. 12. CVs of (A) Co oxide (B) Ni oxide (C) Co-Ni oxide electrodes: curve (1) 146 mM-2.5 M KOH and curve (2) 2.5 M KOH electrolyte solution; scan +50-600 mV, scan rate  $50 \text{ mV s}^{-1}$ .

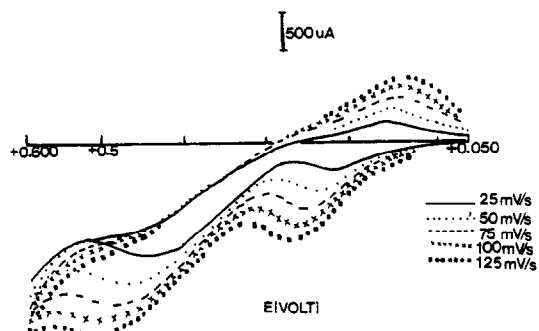


Fig. 13. CVs of Co-Ni oxide electrode; 146 mM ethanol-2.5 M KOH solution scan rate dependence: (---)  $25 \text{ mV s}^{-1}$ , (.....)  $50 \text{ mV s}^{-1}$ , (-----)  $75 \text{ mV s}^{-1}$ , (-·-)  $100 \text{ mV s}^{-1}$ , (■)  $125 \text{ mV s}^{-1}$ .

potentials rather than a limiting plateau seen in the hydrodynamic voltammogram of Fig. 5. Plots of peak current at both +0.24 and +0.43 V vs. scan rate or (scan rate)<sup>1/2</sup> were inconclusive with respect to mechanism as both were linear within experimental error[35].

### CONCLUSION

Electrodeposition has been successfully used to form a mixed Co–Ni oxide film which catalyses the oxidation of aqueous ethanol at very low potentials. Experimental parameters have been varied to determine the optimum catalytic efficiency of the mixed oxide film. This film is used as a detector for the analysis of aqueous ethanol in the amperometric mode in a concentration range of 1.5 mM to 79 mM with a detection limit of 32  $\mu$ M under the experimental conditions of this study. The results presented indicate that the sensitivity of this sensor could be lowered by two or more orders of magnitude simply by decreasing the cell volume, and increasing the electrode area and the applied analytical potential of the electrode to +0.43 V (see Fig. 12C). Preliminary experiments indicate that the lifetime of this electrode is greatly extended by a dynamic continuous ethanol oxidation mode on storage rather than the usual rest mode used for most electrode sensors. Deposition condition variations, EDAX and electrochemical kinetic studies suggest that 2:1 Co–Ni oxide species is the active species in the film which is consistent with results reported in the literature for Co–Ni oxide catalytic electrodes produced by a high temperature process[32].

*Acknowledgements*—This research was supported in part by a grant from Philip Morris International and by the Department of Chemistry, University of Cincinnati. One of us (ETH) is grateful for Patricia Robert Harris graduate fellowships. A. G. thanks Professors S. A. Darwish and M. W. Khalil for this support. We also thank Ernest Clark (Department of Materials Sciences, College of Engineering, U.C.) for SEM and EDAX measurements and the helpful discussion of W. R. Heineman (Department Chemistry, U. C.) and D. E. Leyden (Philip Morris).

### REFERENCES

1. B. D. McNicol, *J. electroanal. Chem.* **118**, 71 (198).
2. J. B. Goodenough, A. Hamnett, B. J. Kennedy, R. Manoharan and S. A. Weks, *J. electroanal. Chem.* **240**, 133 (1988).
3. V. S. Bagotzky and Yu. B. Vassilyer, *Electrochim. Acta* **12**, 1323 (1967).
4. V. S. Bagotzky, Yu. B. Vassilyer and D. A. Khazova, *J. electroanal. Chem.* **81**, 229 (1977).
5. F. Lazaro, M. D. Luque de Castro and M. Valcarcel, *Microchem. J.* **36**, 185 (1987).
6. F. Tagliaro, D. DeLeo, M. Marigo, R. Dorizai and G. Schiavon, *Biomedical Chromatogr.* **4**, 224 (1990).
7. J. Ruz, M. Delores Luque de Castro and M. Valcarcel, *Analyst* **112**, 259 (1987).
8. W. J. Albery, P. N. Bartlett, A. E. G. Cass and K. W. Sim, *J. electroanal. Chem.* **218**, 127 (1987).
9. G. G. Guilbault, B. Danielsson, C. F. Mandenius and K. Mosbach, *Anal. Chem.* **55**, 1582 (1983).
10. P. C. Biswas and M. Enyo, *J. electroanal. Chem.* **322**, 203 (1992).
11. G. Roslonek and J. Taraszewska, *J. electroanal. Chem.* **325**, 285 (1992).
12. M. Beley, J. P. Collin, R. Ruppert and J. P. Sauvage, *J. Am. chem. Soc.* **108**, 746 (1986).
13. F. Beck and H. Schulz, *Electrochim. Acta* **29**, 1569 (1984).
14. J. P. Collins, a. Jouaiti and J. P. Sauvage, *Inorg. Chem.* **292**, 1886 (1988).
15. M. M. P. Janssen and J. Moolhuysen, *Electrochim. Acta* **21**, 869 (1976).
16. B. Beden, F. Kadirgan, C. Lamy and J. M. Leger, *J. electroanal. Chem.* **121**, 343 (1981).
17. M. Fleischmann, K. Korinek and D. Pletcher, *J. electroanal. Chem.* **31**, 39 (1971).
18. H. J. Schafer, *Top. Curr. Chem.* **142**, 101 (1986).
19. S. Torii, *electroorganic Syntheses—Methods and Applications*, Part 1, p. 341. VCH Kodansha (1985).
20. A. C. C. Tseung and S. Jasem, *Electrochim. Acta* **22**, 31 (1977).
21. A. C. C. Tseung and S. Jasem, *Electrochim. Acta Soc.* **129**, 515 (1982).
22. R. Parson, *Trans. Faraday Soc.* **54**, 1053 (1958).
23. D. Pletcher, *J. appl. Electrochem.* **20**, 403 (1984).
24. L. C. Jiang and D. Pletcher, *J. electroanal. Chem.* **149**, 237 (1983).
25. M. Fleischmann, J. Koryta and H. R. Thirsk, *Trans. Faraday Soc.* **63**, 1261 (1967).
26. M. Fleischmann, J. Koryta and H. R. Thirsk, *Trans. Faraday Soc.* **68**, 2305 (1972).
27. E. Yeager, W. O'Grady, M. Woo and P. Hagens, *J. electrochem. Soc.* **125**, 348 (1978).
28. J. Clavilier, R. Parsons, R. Durand, c. Lamk and J. W. Ledger, *J. electroanal. Chem.* **124**, 321 (1981).
29. P. Cox and D. Pletcher, *J. appl. Electrochem.* **20**, 549 (1990).
30. J. Haensen, W. Visscher and E. Barendrecht, *J. electroanal. Chem.* **208**, 273 (1986).
31. A. Capron and R. Parsons, R. Durand, C. Larry and J. W. Leger, *J. electroanal. Chem.* **45**, 205 (1973).
32. J. Haensen, W. Vischer and E. Barendrecht, *J. electroanal. Chem.* **208**, 297 (1986).
33. J. D. Ingle Jr and S. R. Crouch, *Spectrochemical Analysis*, pp. 172–176. Prentice Hall, Englewood Cliffs, NJ (1988).
34. H. B. Mark Jr and G. A. Rechnitz, *Kinetics in Analytical Chemistry*, pp. 67–68. Interscience New York (1968).
35. A. J. Bard and L. R. Faulkner, *Electrochemical Methods*, Chap. 11, pp. 521–532 Wiley, New York (1980).